AIP | The Journal of Chemical Physics

Exploiting adiabatically switched RF-field for manipulating spin hyperpolarization induced by parahydrogen

Alexey S. Kiryutin, Alexandra V. Yurkovskaya, Nikita N. Lukzen, Hans-Martin Vieth, and Konstantin L. Ivanov

Citation: The Journal of Chemical Physics **143**, 234203 (2015); doi: 10.1063/1.4937392
View online: http://dx.doi.org/10.1063/1.4937392
View Table of Contents: http://scitation.aip.org/content/aip/journal/jcp/143/23?ver=pdfcov
Published by the AIP Publishing

Exploiting adiabatically switched RF-field for manipulating spin hyperpolarization induced by *para*hydrogen

Alexey S. Kiryutin,[1,2] Alexandra V. Yurkovskaya,[1,2] Nikita N. Lukzen,[1,2]
Hans-Martin Vieth,[1,3] and Konstantin L. Ivanov[1,2,a)]
[1]*International Tomography Center SB RAS, Institutskaya 3a, Novosibirsk 630090, Russia*
[2]*Novosibirsk State University, Pirogova 2, Novosibirsk 630090, Russia*
[3]*Freie Universität Berlin, Arnimallee 14, Berlin 14195, Germany*

(Received 30 September 2015; accepted 5 November 2015; published online 21 December 2015)

A method for precise manipulation of non-thermal nuclear spin polarization by switching a RF-field is presented. The method harnesses adiabatic correlation of spin states in the rotating frame. A detailed theory behind the technique is outlined; examples of two-spin and three-spin systems prepared in a non-equilibrium state by *Para*-Hydrogen Induced Polarization (PHIP) are considered. We demonstrate that the method is suitable for converting the initial multiplet polarization of spins into net polarization: compensation of positive and negative lines in nuclear magnetic resonance spectra, which is detrimental when the spectral resolution is low, is avoided. Such a conversion is performed for real two-spin and three-spin systems polarized by means of PHIP. Potential applications of the presented technique are discussed for manipulating PHIP and its recent modification termed signal amplification by reversible exchange as well as for preparing and observing long-lived spin states. © *2015 AIP Publishing LLC.* [http://dx.doi.org/10.1063/1.4937392]

I. INTRODUCTION

Para-Hydrogen Induced Polarization (PHIP)[1–3] is a popular method for creating non-equilibrium polarization of nuclear spins thereby boosting weak Nuclear Magnetic Resonance (NMR) signals. PHIP is based on using *para*hydrogen, i.e., the H_2 molecule in its nuclear singlet state, which can be prepared by performing spin conversion in the H_2 gas at low temperature. To form observable spin magnetization from the otherwise NMR silent *para*hydrogen, it is necessary to exploit a chemical reaction, which breaks the symmetry of the two protons. For this purpose, catalytic hydrogenation reactions are used; in such reactions, *para*-H_2 is attached to a substrate with a double or triple C–C bond.

The two traditional ways to run PHIP experiments are termed PASADENA (*Para*hydrogen and Synthesis Allow Dramatically Enhanced Nuclear Alignment) and ALTADENA (Adiabatic Longitudinal Transport After Dissociation Engenders Net Alignment). In PASADENA experiments,[4] the hydrogenation reaction is run directly at the high magnetic field of a NMR spectrometer; in the ALTADENA case,[5] *para*hydrogen is attached to the substrate at low field (presumably, the earth field); subsequently the polarized reaction product is transported to the high detection field where the NMR spectrum is taken. In both cases, one obtains strongly enhanced NMR lines of the reaction product although the appearance of the spectra is different. The PASADENA pattern consists of two anti-phase doublets; whereas in the ALTADENA case, the two protons also acquire net polarization of the same amplitude but of opposite sign. More recently, an important modification of PHIP has been developed, which is termed Signal Amplification By Reversible Exchange (SABRE).[6] The SABRE method exploits transfer of the spin order of *para*hydrogen to a substrate in a transient complex. Optimizing the efficiency of such a transfer is crucial for the performance of SABRE. Typically, spin order transfer to a third spin is efficient at low magnetic fields;[6,7] however, very recently, it has been demonstrated that SABRE is operative at high magnetic fields, when the spin system is excited by resonant RF-fields[8,9] providing strong signal enhancements of the spins of substrates.

Both schemes of the standard PHIP experiment, PASADENA and ALTADENA, are widely used in modern NMR;[1–3] however, the range of potential PHIP applications can be limited by the fact that despite the strong signal enhancement of individual NMR lines, the total intensity of PHIP spectra integrated over all lines is zero, i.e., no net signal polarization is present. This does not create any problems in high-resolution NMR, i.e., when the spectral lines do not overlap, but imposes serious limitations for low-resolution studies. This is often the case when field inhomogeneity is present, e.g., in NMR imaging experiments. There are several ways to tackle the problem of low spectral resolution, for example, by converting[10] the anti-phase spin order into net polarization or by using spin echo techniques[11–13] and specially designed pulse sequences to separate thermal polarization and PHIP.[14,15] Recently, we have proposed a method,[16] which is also suitable for the purpose of avoiding signal cancellation in PHIP. This method is based on running the hydrogenation reaction at high field in the presence of a strong resonant RF-field, a spin-locking field. After forming the polarized reaction product, the RF-field is reduced to zero

a)Author to whom correspondence should be addressed. Electronic mail: ivanov@tomo.nsc.ru. Telephone: +7(383)330-8868. Fax: +7(383)333-1399.

in an adiabatic fashion. We have demonstrated that in this experiment, the anti-phase spin order can be converted with high efficiency into net polarization. Furthermore, by varying the RF-frequency, one can precisely manipulate the spectral pattern in a desirable way: depending on the frequency, it is possible to obtain ALTADENA-like spectra, to invert the PASADENA spectral pattern and, most notably, to net-polarize both spins positively or negatively. It is worth noting that in this method, there is only conversion of the initial singlet spin order and no loss of spin order. We have also presented a theoretical treatment of the problem and demonstrated that the method works experimentally taking a two-spin system polarized by PHIP.[16] In general, methods using adiabatic variation of the spin Hamiltonian are frequently used in magnetic resonance[17–25] and can be successfully applied to manipulate spin hyperpolarization.[16,26,27]

In this work, we would like to present further development of the method. First, we describe the theory in more detail and present theoretical results for two-spin and three-spin systems. We argue that the method is applicable to more than two coupled spins, which is crucial, for instance, for SABRE experiments. Second, we discuss conditions for RF switching, specifically, times compatible with adiabatic variation of the Hamiltonian. Third, we present new experimental results showing that the method is very helpful for low-resolution studies. Finally, we demonstrate that three-spin systems can be efficiently net-polarized with this method and that PHIP can be transferred from a pair of primarily polarized protons to a third spin. Experiments are done for polarized ethyl cinnamate and styrene, which contain a polarized two-spin and three-spin system, respectively. Here, all results are obtained for the traditional PHIP, although we anticipate that this technique can be applied to SABRE as well. We restrict ourselves to PHIP for the sake of clarity; possible generalization of the technique is discussed in the Conclusions.

II. THEORY

A. General expressions

In the theoretical description, we always refer to the following experimental protocol, see Figure 1, also used[16] in our earlier work. We assume that polarization is prepared at a high magnetic field B_0 and also in the presence of a resonance spin-locking RF-field, which is turned on for the period of time τ_{SL}. Here, we used two different options for spin-locking: (i) turning on strong RF-field using a constant power level or (ii) using the WALTZ-16 pulse sequence, which has a better performance as far as excitation of a broad NMR spectrum is concerned.[28,29] After the preparation, the RF-field is slowly (adiabatically) turned off during the time period τ_{off}. We will explain below what is meant here by adiabatic reduction of the RF-field. Finally, a detecting RF-pulse with a flip angle φ is applied to obtain the Free Induction Decay (FID) signals; the NMR spectrum of the spin system is the Fourier transform of the FID.

During the preparation period, a system of N coupled spins-1/2 is described by the following Hamiltonian in the RF-rotating frame of reference (in units of h):

$$\hat{H}_{0,rf} = -\sum_{i=1}^{N} \delta\nu_i \hat{I}_{iz} - \nu_1^0 \sum_{i=1}^{N} \hat{I}_{ix} + \sum_{i\neq j}^{N} J_{ij} \left(\hat{\mathbf{I}}_i \cdot \hat{\mathbf{I}}_j\right), \quad (1)$$

where $\delta\nu_i = (\nu_i - \nu_{rf})$ with ν_i being the NMR frequency of the ith spin at field B_0 given by its chemical shift δ_i; ν_{rf} and ν_1^0 are the RF-field frequency and its starting amplitude, respectively; J_{ij} are the scalar couplings for all pairs of spins. As usually done in PHIP, we assume that the preparation lasts for a rather long period of time, such that all spin coherences (in the eigen-basis of the spin Hamiltonian) are washed out. Thus, to construct the density matrix, ρ_0, of the spin system prior to the reduction of the RF-field, we proceed as follows. First, we construct the density matrix, ρ_s, describing spin 1 and spin 2 in their singlet state (hereafter, we always assume that spin 1 and spin 2 are those originating from *para*hydrogen) and the other spins non-polarized,

$$\rho_0 = \rho_s(12) \otimes \rho_{eq}(3) \otimes \cdots \otimes \rho_{eq}(N). \quad (2)$$

Here,

$$\rho_s = \begin{pmatrix} 0 & 0 & 0 & 0 \\ 0 & 1/2 & -1/2 & 0 \\ 0 & -1/2 & 1/2 & 0 \\ 0 & 0 & 0 & 0 \end{pmatrix}, \quad \rho_{eq}(i) = \begin{pmatrix} 1/2 & 0 \\ 0 & 1/2 \end{pmatrix}, \quad (3)$$

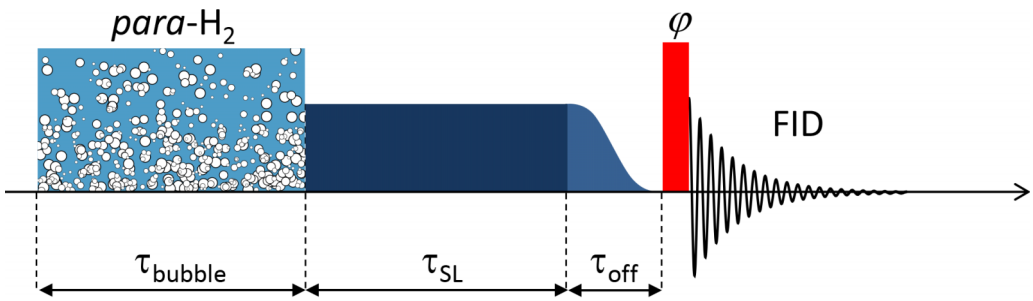

FIG. 1. Protocol of the PHIP experiment with adiabatic fading of the RF-field. The experiment is performed at a high magnetic field B_0. First, the sample is bubbled with *para*hydrogen during a time period τ_{bubble}; subsequently, a strong RF-field (spin-locking) is turned on for a time period τ_{SL}. After preparation of non-thermal spin order under spin-locking conditions, the RF-field is turned off during the time τ_{off} and the Free Induction Decay (FID) signal is detected after applying a NMR pulse with magnetization flip angle φ.

the spins are listed in parentheses. After introducing ρ_s, we solve the eigen-problem of the Hamiltonian $\hat{H}_{rf}$,

$$\hat{T}^{-1}\hat{H}_{0,rf}\hat{T} = \hat{\Lambda}, \tag{4}$$

where $\hat{\Lambda}$ is a diagonal matrix with matrix elements giving the energy levels, E_μ^{rf}, in the rotating frame: $\Lambda_{\mu\nu} = \delta_{\mu\nu}E_\mu^{rf}$ (here $\delta_{\mu\nu}$ is the Kronecker delta) and $\hat{T}$ is the matrix of eigen-vectors of $\hat{H}_{0,rf}$. Then, we write ρ_s in the new basis,

$$\hat{T}^{-1}\rho_0\hat{T} = \rho_0^{eb}. \tag{5}$$

In the new matrix, ρ_s^{eb}, we remove all off-diagonal elements (spin coherences) and obtain the density matrix at the end of the preparation stage as $\sigma = Diag(\rho_0^{eb})$. We would like to mention (as a caveat) that this procedure is valid only for non-degenerate energy eigenstates. The diagonal matrix elements of σ (state populations) are[30,31]

$$p_\mu = \sigma_{\mu\mu} = |\langle\mu|S_{12}\rangle|^2, \tag{6}$$

where $|\mu\rangle$ is the μth eigen-state of $\hat{H}_{0,rf}$ and $|S_{12}\rangle$ is the singlet state of spins 1 and 2. Setting spin coherences equal to zero is usually a valid assumption in PHIP because the polarized molecules are continuously produced in a relatively slow chemical reaction.[30]

The next step in calculating the spin dynamics is considering the evolution of the spin density matrix σ during reduction of the RF-field, i.e., under the action of a time-dependent Hamiltonian in the rotating frame. To describe this evolution, we solve the Liouville-von Neumann equation

$$\dot{\sigma}(t) = -2\pi i\left[\hat{H}_{rf}(t), \sigma(t)\right], \tag{7}$$

where

$$\hat{H}_{rf}(t) = -\sum_{i=1}^{N}\delta\nu_i\hat{I}_{iz} - \nu_1(t)\sum_{i=1}^{N}\hat{I}_{ix} + \sum_{i\neq j}^{N}J_{ij}\left(\hat{I}_i\cdot\hat{I}_j\right). \tag{8}$$

The time dependence is due to the variation of the RF-field strength, $\nu_1(t)$, from $\nu_1(t=0) = \nu_1^0$ to $\nu_1\left(t=\tau_{off}\right) = 0$. We solve this equation either numerically by splitting the time interval $[0, \tau_{off}]$ in many small steps (calculating the evolution assuming time-independent Hamiltonian within each step) or analytically under the assumption of adiabatic variation of the Hamiltonian $\hat{H}_{rf}(t)$. By adiabatic variation, we assume that the state populations have enough time to adjust themselves to the eigen-states of $\hat{H}_{rf}(t)$, which change with time. That is, populations always follow the states. The adiabaticity criterion can be formulated in terms of the following quantities:[32]

$$\xi_{\mu\nu}(t) = \left|\frac{\alpha_{\mu\nu}(t)}{2\pi\delta E_{\mu\nu}(t)}\right|. \tag{9}$$

Here, the quantities $\alpha_{\mu\nu}$ and $\delta E_{\mu\nu}$ are introduced via the solution of the eigen-problem of $\hat{H}_{rf}(t)$,

$$\hat{H}_{rf}(t)|\mu\rangle(t) = E_\mu(t)|\mu\rangle(t) \tag{10}$$

as

$$\alpha_{\mu\nu}(t) = \langle\mu|\frac{d|\nu\rangle}{dt},\ \delta E_{\mu\nu}(t) = E_\mu(t) - E_\nu(t). \tag{11}$$

When $\xi_{\mu\nu}(t) \ll 1$, i.e., the eigen-states change very slowly as compared to the frequencies of internal evolution of the system, the variation of $\hat{H}_{rf}(t)$ is adiabatic; in the opposite case, the switching is sudden. For a general spin system, it is relatively difficult to formulate the adiabaticity criterion analytically. In fact, in the presence of a RF-field, this is hard to do already for a two-spin system, since there are four mixed states involved. Therefore, we study the adiabaticity issue separately by running experiments and calculations with different times and profiles of RF fading. For a two-spin system, the minimal time compatible with adiabatic switching is roughly given by the inverse spin-spin coupling, $1/J_{12}$ (*vide infra*). As we see later, comparison of experiments and theory shows that our calculation method is appropriate for estimating the degree of adiabaticity; therefore, in a more general case, one can use such calculations to evaluate the RF fading times compatible with adiabatic variation of $\hat{H}_{rf}(t)$.

In the situation of adiabatic variation of $\hat{H}_{rf}(t)$, to calculate spin evolution it is sufficient to (i) find the eigen-states $|\mu\rangle$ of $\hat{H}_{0,rf}$ and their populations, p_μ, at strong ν_1^0, (ii) group the states in the order of ascending (or descending) energy, (iii) do the same for the states at $\nu_1 = 0$, and (iv) perform the correlation of states. The latter means that after RF fading the lowermost energetic state at $\nu_1 = 0$ has the same population as the lowermost state of $\hat{H}_{0,rf}$; the second lowest state at $\nu_1 = 0$ acquires the population of the second lowest state of $\hat{H}_{0,rf}$, and so on. When the switching is adiabatic, no spin coherences are formed; coherences should be considered in the case of non-adiabatic variation of the Hamiltonian as has been described in detail in Ref. 33. Here, we focus on the adiabatic case. We demonstrate in the Subsections II B and II C how correlation of adiabatic states is performed for two-spin and three-spin systems, stressing that correlation is always performed in the rotating frame of reference.

The final stage of the calculation is computing the Fourier-transform NMR spectrum, which has a non-trivial dependence[34,35] on the magnetization flip angle used for detection. We will use the same method of calculating spectra of hyperpolarized spins as before;[16,33] the method is valid for arbitrary flip angles φ and is also suitable for calculating the spectra in the presence of spin coherences.

Now, let us discuss the theoretical results for two-spin and three-spin systems.

B. Two-spin system

In the case of two coupled spins, the eigen-problem of the Hamiltonian can be solved for very large ν_1 and for zero ν_1; this is sufficient for our purposes. In the case of very strong ν_1, the spins are quantized along the x-axis and are characterized by the total spin and its projection on the x-axis, i.e., the RF-field direction in the rotating frame. By a "very strong" RF-field, we mean that the precession frequencies of the two spins about their effective fields in the rotating frame are almost the same. More specifically, the effective precession frequencies of the two spins are

$$\nu_{1,2}^{eff} = \sqrt{(\delta\nu_{1,2})^2 + \left(\nu_1^0\right)^2}. \tag{12}$$

At very strong RF-fields, the difference, $\left|\nu_1^{eff} - \nu_2^{eff}\right|$, becomes much smaller than $|J_{12}|$. Indeed, at $\nu_1^0 \gg |\delta\nu_{1,2}|$, the effective

fields are almost parallel to the x-axis; furthermore, we obtain at large ν_1^0,

$$\nu_1^{eff} - \nu_2^{eff} \approx \frac{1}{2\nu_1^0}\left[(\delta\nu_1)^2 - (\delta\nu_2)^2\right] \ll J_{12}. \quad (13)$$

When these conditions are fulfilled, the Hamiltonian $\hat{H}_{0,rf}$ is simplified as

$$\hat{H}_{0,rf} \approx -\nu_1^0\left(\hat{I}_{1x} + \hat{I}_{2x}\right) + J_{12}\left(\hat{\mathbf{I}}_1 \cdot \hat{\mathbf{I}}_2\right). \quad (14)$$

The eigen-states of this Hamiltonian are the singlet state, $|S\rangle$, and three triplet states, $|T_+\rangle$, $|T_0\rangle$, and $|T_-\rangle$. One should note, however, that the triplet states should be written in the basis, where the projection of the total spin along the x-axis is defined but not the z-projection (as it is usually done). Consequently, these $|T_\pm\rangle$ triplet states do not coincide with the $|\alpha\alpha\rangle$ and $|\beta\beta\rangle$ states, i.e., the states characterized by a definite projection of the total spin on the z-axis (parallel to the B_0 field). However, in our case, it does not impose any additional complications because due to the singlet-state preparation, the triplet states stay empty and we only need to calculate their energies. The energies of the four states are

$$\begin{aligned} E_S^{rf} &= -\frac{3}{4}J_{12},\ E_{T_0}^{rf} = \frac{1}{4}J_{12}, \\ E_{T_+}^{rf} &= -\nu_1^0 + \frac{1}{4}J_{12},\ E_{T_-}^{rf} = \nu_1^0 + \frac{1}{4}J_{12}. \end{aligned} \quad (15)$$

That is, when $J_{12} > 0$ (which is usually the case in PHIP), the singlet state is always the state second lowest in energy.

When the RF-field is reduced to zero, the Hamiltonian of the two-spin system in the rotating frame is

$$\hat{H}_0 = -\delta\nu_1\hat{I}_{1z} - \delta\nu_2\hat{I}_{2z} + J_{12}\hat{I}_{1z}\hat{I}_{2z}. \quad (16)$$

Here, we assume weak coupling of spins in the absence of spin-locking, which allows us to omit the non-secular terms in the spin-spin interaction. The solution of the eigen-problem of such Hamiltonian is straightforward: the eigen-states are the Zeeman states, $|\alpha\alpha\rangle$, $|\alpha\beta\rangle$, $|\beta\alpha\rangle$, and $|\beta\beta\rangle$; their energies are

$$\begin{aligned} E_{\alpha\alpha} &= -\frac{\delta\nu_1}{2} - \frac{\delta\nu_2}{2} + \frac{J_{12}}{4},\ E_{\alpha\beta} = -\frac{\delta\nu_1}{2} + \frac{\delta\nu_2}{2} - \frac{J_{12}}{4}, \\ E_{\beta\alpha} &= \frac{\delta\nu_1}{2} - \frac{\delta\nu_2}{2} - \frac{J_{12}}{4},\ E_{\beta\beta} = \frac{\delta\nu_1}{2} + \frac{\delta\nu_2}{2} + \frac{J_{12}}{4}. \end{aligned} \quad (17)$$

Interestingly, in the rotating frame (in contrast to the lab frame), the $|\alpha\alpha\rangle$ and $|\beta\beta\rangle$ states are not necessarily the lowermost and uppermost energetic states. In fact, the order of states is determined by the sign of $\delta\nu_1$ and $\delta\nu_2$, which, in turn, depends on the position of the RF-frequency, ν_{rf}, with respect to the spectral lines, i.e., with respect to ν_1 and ν_2. This significantly affects the correlation of adiabatic states of $\hat{H}_{rf}(t)$, which is performed in the rotating frame but not in the lab frame (where fast oscillating terms are present in the Hamiltonian originating from the RF-fields). As a consequence, the singlet state (populated under spin-locking conditions) is correlated with different spin states in the absence of RF-field depending on the sign of $\delta\nu_1$ and $\delta\nu_2$. Changing the sign of $\delta\nu_1$ and $\delta\nu_2$ by varying ν_{rf} and correlating the states in the rotating frame are in the heart of our method of manipulating the singlet spin order in PHIP and changing the spectral pattern in a desirable way by simply varying ν_{rf}.

The sign of $\delta\nu_i$ changes when ν_{rf} "passes through" the NMR frequency, ν_i, of the corresponding spin; consequently, at $\nu_{rf} = \nu_1$ and $\nu_{rf} = \nu_2$, the resulting spectral pattern changes. In addition, the order of states changes when $\nu_{rf} = \langle\nu\rangle = (\nu_1 + \nu_2)/2$, i.e., when ν_{rf} "passes through" the center of gravity of the NMR spectrum. At these three spectral positions, ν_1, ν_2, and $\langle\nu\rangle$ (regime switching positions), the correlation of adiabatic states changes as well as the NMR spectrum detected after switching off the RF-field.

Analytical results for all different situations, which appear for a two-spin system, are given in the supplementary materials;[36] PHIP spectra for different cases, i.e., for different ν_{rf} values, have been calculated in Ref. 16 and experimentally demonstrated there. In Figure 2, we give a brief summary of these results by showing the dependence of the relevant spin operators on the frequency ν_{rf}. These spin operators are net polarizations of the two spins, $\langle I_{1z}\rangle = Tr\{\hat{I}_{1z}\sigma\}$ and $\langle I_{2z}\rangle = Tr\{\hat{I}_{2z}\sigma\}$, and two-spin order (multiplet polarization), $\langle I_{1z}I_{2z}\rangle = Tr\{\hat{I}_{1z}\hat{I}_{2z}\sigma\}$.

All calculations for a two-spin system are done here for the NMR parameters, which correspond to those of ethyl cinnamate:

$$\begin{aligned} &\text{chemical shifts are } \delta_1 = 7.0165 \text{ ppm and } \delta_2 = 5.994 \text{ ppm;} \\ &\text{J-coupling is } J_{12} = 12.74 \text{ Hz.} \end{aligned} \quad (18)$$

Depending on the RF-frequency, one can transfer the singlet state population into a particular Zeeman state of choice and

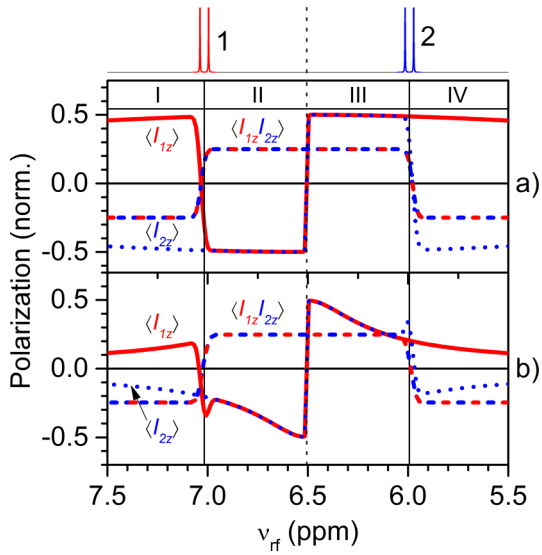

FIG. 2. Dependence of polarization on the RF-frequency, ν_{rf}, calculated for a two-spin system. Here, net polarization of spins is shown, $\langle I_{1z}\rangle$ (solid red lines) and $\langle I_{2z}\rangle$ (dotted blue lines), as well as multiplet polarization, $\langle I_{1z}I_{2z}\rangle$ (dashed red-blue lines). Calculation parameters: NMR parameters are taken from Eq. (18); the static magnetic field is $B_0 = 9.4$ T. The RF-field is slowly reduced from a high initial value, the switching time profile is $\nu_1(t) = \nu_1^0\cos^2(\pi t/2\tau_{off})$; in (a), $\nu_1^0 = 30$ kHz, $\tau_{off} = 3$ s; in (b), $\nu_1^0 = 3$ kHz, $\tau_{off} = 1$ s. The calculated thermal NMR spectrum is shown on top; thin vertical lines show the NMR frequencies of the two spins (solid lines) and the center of the spectrum (dashed line). Numbers I-IV indicate the four different regimes of adiabatic correlation of states in the rotating frame: $S \to \alpha\beta$ (I), $S \to \beta\beta$ (II), $S \to \alpha\alpha$ (III), and $S \to \alpha\beta$ (IV).

thus manipulate the spectral pattern. The different regimes of adiabatic state correlation are indicated in Figure 2. Importantly, it is possible to net-polarize the spin system: In the cases (II) and (III), the singlet state population selectively goes to $|\beta\beta\rangle$ and $|\alpha\alpha\rangle$, respectively, see Figure 2. During the RF-field switching, there is no loss of spin order but only conversion: Depending on ν_{rf}, the initial singlet state population is completely transferred to $|\alpha\alpha\rangle$, $|\beta\beta\rangle$, or $|\alpha\beta\rangle$ (except for the cases $\nu_{rf} = \nu_1, \nu_2, \langle\nu\rangle$ in which the singlet state population is shared between a pair of Zeeman states). At $\nu_{rf} = \nu_1, \nu_2, \langle\nu\rangle$, there are abrupt stepwise features in the curves corresponding to the changes in correlation of adiabatic states in the rotating frame.

In the calculation, we assume that PHIP is prepared under strong RF-field with $\nu_1^0 = 30$ kHz, which is slowly reduced with the following time profile: $\nu_1(t) = \nu_1^0 \cos^2(\pi t/2\tau_{off})$, which provides a smooth decrease of the RF-field amplitude to zero; the time τ_{off} is also taken relatively long. In the limit of complete adiabaticity (which is, in fact, never met in real experiments), the stepwise features have zero width; in reality, this width is never zero but is finite. However, with the parameters chosen, it is possible to set the RF-frequency and the τ_{off} time such that all the regimes of state correlation discussed above are indeed met. When we take more moderate parameters, i.e., a lower ν_1^0 value and shorter τ_{off}, one can see deviations from the idealized case, see Figure 2(b). Specifically, the regions where there are changes in the correlation of adiabatic states become broader and the efficiency of spin order conversion becomes lower. In addition, in the frequency dependences of $\langle I_{1z}\rangle$ and $\langle I_{2z}\rangle$, there are additional peaks at $\delta\nu_{1,2} = 0$. However, the overall performance of the method is good: It is possible to reach the values of polarization $\langle I_{1z}\rangle, \langle I_{2z}\rangle$ of about $\pm\frac{1}{2}$ by properly setting ν_{rf}.

C. Three-spin system

The case of three coupled spins is more complex but can still be analyzed in a similar way. When the RF-field, ν_1^0, is sufficiently strong, we can approximately write the Hamiltonian $\hat{H}_{0,rf}$ as

$$\hat{H}_{0,rf} \approx -\nu_1^0\left(\hat{I}_{1x} + \hat{I}_{2x} + \hat{I}_{3x}\right) + J_{12}\left(\hat{\mathbf{I}}_1 \cdot \hat{\mathbf{I}}_2\right) + J_{12}\left(\hat{\mathbf{I}}_1 \cdot \hat{\mathbf{I}}_3\right) + J_{12}\left(\hat{\mathbf{I}}_2 \cdot \hat{\mathbf{I}}_3\right). \quad (19)$$

The eigen-states of such Hamiltonian are characterized by the total spin, I, which takes the values of $I = \frac{1}{2}$ and $I = \frac{3}{2}$, and its projection on the effective field axis, i.e., on the x-axis. These states are $|1\rangle = |\frac{3}{2}, \frac{3}{2}\rangle$, $|2\rangle = |\frac{3}{2}, \frac{1}{2}\rangle$, $|3,4\rangle = |\frac{1}{2}, \frac{1}{2}\rangle$, $|5,6\rangle = |\frac{1}{2}, -\frac{1}{2}\rangle$, $|7\rangle = |\frac{3}{2}, -\frac{1}{2}\rangle$, and $|8\rangle = |\frac{3}{2}, -\frac{3}{2}\rangle$ (like in the previous case, one should bear in mind that the quantization axis is not z but x). The energies of these states are:[37,38]

$$\begin{aligned} E_1 &= -\frac{3}{2}\nu_1^0 + \frac{1}{4}\Sigma, \quad E_2 = -\frac{1}{2}\nu_1^0 + \frac{1}{4}\Sigma, \\ E_{3,4} &= -\frac{1}{2}\nu_1^0 - \frac{1}{4}\Sigma \pm \frac{1}{2}\Gamma, \quad E_{5,6} = \frac{1}{2}\nu_1^0 - \frac{1}{4}\Sigma \pm \frac{1}{2}\Gamma, \\ E_7 &= \frac{1}{2}\nu_1^0 + \frac{1}{4}\Sigma, \quad E_8 = \frac{3}{2}\nu_1^0 + \frac{1}{4}\Sigma. \end{aligned} \quad (20)$$

Here $\Sigma = J_{12} + J_{13} + J_{23}$, $\Gamma = \sqrt{\Sigma^2 - 3\Theta}$, and $\Theta = J_{12}J_{13} + J_{12}J_{23} + J_{13}J_{23}$. When $\Sigma > \Gamma > 0$ (which is usually the case), the energies are ordered in the following way:

$$E_1 < E_4 < E_3 < E_2 < E_6 < E_5 < E_7 < E_8. \quad (21)$$

When singlet state preparation is assumed, only four states, namely, $|3,4\rangle$ and $|5,6\rangle$ characterized by the total spin $I = \frac{1}{2}$, out of eight are populated; their populations are[37,38]

$$\begin{aligned} p_3 = p_5 = p_+ &= \frac{1}{4}\left(c_a^+ - c_b^+\right)^2, \\ p_4 = p_6 = p_- &= \frac{1}{4}\left(c_a^- - c_b^-\right)^2, \end{aligned} \quad (22)$$

where

$$c_a^\pm = \frac{J_{13} - J_{23} \pm \Gamma}{\Upsilon_\pm}, \; c_b^\pm = \frac{J_{12} - J_{13}}{\Upsilon_\pm}, \\ \Upsilon_\pm = \sqrt{(J_{12} - J_{13})^2 + (J_{12} - J_{23} \pm \Gamma)^2 + (J_{13} - J_{23} \pm \Gamma)^2}. \quad (23)$$

To obtain the state populations after reduction of the RF-field, it is again necessary to list (in ascending or descending order) the states of the Hamiltonian,

$$\hat{H}_0 = \delta\nu_1\hat{I}_{1z} - \delta\nu_2\hat{I}_{2z} - \delta\nu_3\hat{I}_{3z} + J_{12}\hat{I}_{1z}\hat{I}_{2z} + J_{13}\hat{I}_{1z}\hat{I}_{3z} + J_{23}\hat{I}_{2z}\hat{I}_{3z}. \quad (24)$$

Here, we will not discuss all possible regimes of correlation of adiabatic states in the rotating frame because there are too many of them. Indeed, there are several positions, ν_{rf}, where the regime switches. These are, for instance, three NMR frequencies, ν_1, ν_2, ν_3, and the "centers of gravity" for each pair of spins, $\frac{\nu_1+\nu_2}{2}$, $\frac{\nu_1+\nu_3}{2}$, $\frac{\nu_2+\nu_3}{2}$. For this reason, we will explain how state correlation should be done in one particular case. We will consider a system of three spins with parameters modeling the three-spin system of styrene, which is characterized by the following chemical shifts and J-couplings:

$$\begin{gathered} \text{chemical shifts are } \delta_1 = 6.765 \text{ ppm}, \delta_2 = 5.243 \text{ ppm}, \text{ and} \\ \delta_3 = 5.80 \text{ ppm} \\ \text{J-couplings are } J_{12} = 10.9 \text{ Hz}, J_{13} = 17.7 \text{ Hz}, \text{ and} \\ J_{23} = 1.0 \text{ Hz} \end{gathered} \quad (25)$$

We consider here two examples, see Figures 3(a) and 3(b): (a) $\nu_1 > \nu_3 > \nu_{rf} > \nu_2$ and also $|\delta\nu_2| < |\delta\nu_3|$; (b) $\nu_1 > \nu_{rf} > \nu_3 > \nu_2$ and also $|\delta\nu_1| < |\delta\nu_3|$.

In both cases, under spin-locking conditions, the levels are grouped with respect to their total spin and its x-projection. When the RF-field is switched off, the states are the Zeeman states in the rotating frame with their energies determined by $\delta\nu_1, \delta\nu_2, \delta\nu_3$. In case (a), the states populated at strong ν_1^0, namely, $|3,4\rangle$ and $|5,6\rangle$, go to the following Zeeman states: $|3\rangle \to |\alpha\beta\beta\rangle, |4\rangle \to |\alpha\alpha\alpha\rangle, |5\rangle \to |\beta\alpha\alpha\rangle, |6\rangle \to |\alpha\alpha\beta\rangle$, which thus acquire the populations of p_+, p_-, p_+, p_-, respectively. The resulting net spin orders are $\langle I_{1z}\rangle = p_-$, $\langle I_{2z}\rangle = p_-$, $\langle I_{3z}\rangle = 0$; that is, the spin system is net-polarized positively: $\langle I_z\rangle = 2p_-$. In case (b), the signs of $\delta\nu_2$ changes as well as the correlation of states: $|3\rangle \to |\alpha\beta\alpha\rangle$, $|4\rangle \to |\beta\beta\beta\rangle$, $|5\rangle \to |\beta\alpha\beta\rangle$) $|6\rangle \to |\beta\beta\alpha\rangle$. In

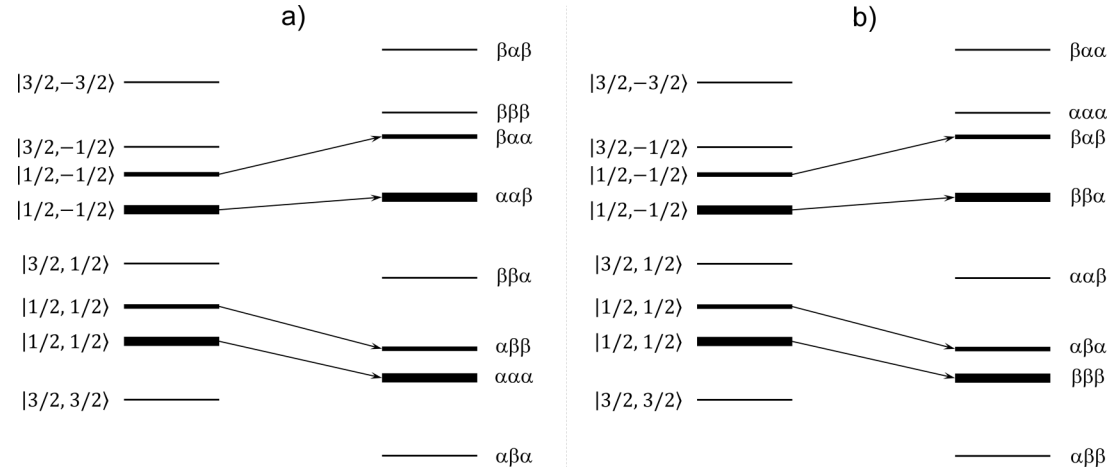

FIG. 3. Correlation of states in a three-spin system in cases (a) $\nu_1 > \nu_3 > \nu_{rf} > \nu_2$ and also $|\delta\nu_2| < |\delta\nu_3|$; (b) $\nu_1 > \nu_{rf} > \nu_3 > \nu_2$ and also $|\delta\nu_1| < |\delta\nu_3|$. In each case, the energy levels at a strong RF-field are shown on the left; the levels at zero RF-field are shown on the right. The thickness of the levels corresponds to their population.

this situation, the spin orders are $\langle I_{1z}\rangle = -p_-$, $\langle I_{2z}\rangle = -p_-$, $\langle I_{3z}\rangle = 0$ and the spin system is net-polarized negatively: $\langle I_z\rangle = -2p_-$.

In Figure 4, we present the complete ν_{rf} -dependence of spin order in the three-spin system discussed. It is readily seen that the behavior is qualitatively similar to that in a two-spin system, even despite a more complex behavior and several ν_{rf} values, at which the polarization pattern is switched. Notably, it is possible to net polarize the spin system and also switch the sign of net and multiplet polarization. In addition, the third spin can be polarized by spin order transfer from spins 1 and 2. The more complex behavior (as compared to a two-spin system) is coming from the larger number of possible state degeneracies

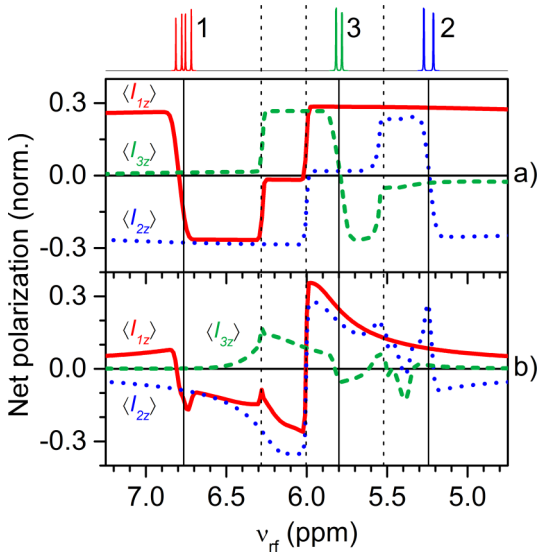

FIG. 4. Dependence of polarization on the RF-frequency, ν_{rf}, calculated for a three-spin system. Here, net polarization of spins is shown, $\langle I_{1z}\rangle$ (solid red lines), $\langle I_{2z}\rangle$ (dotted blue lines), and $\langle I_{3z}\rangle$ (dashed green lines). Calculation parameters: NMR parameters are taken from Eq. (25); the static magnetic field is $B_0 = 9.4$ T. The RF-field is slowly reduced from a high initial value, the switching time profile is $\nu_1(t) = \nu_1^0 \cos^2(\pi t/2\tau_{off})$; in (a), $\nu_1^0 = 30$ kHz, $\tau_{off} = 3$ s; in (b), $\nu_1^0 = 3$ kHz, $\tau_{off} = 1$ s. The calculated thermal NMR spectrum is shown on top; thin vertical lines show the NMR frequencies of the three spins (solid lines) and the centers of gravity of the three pair of spins (dashed lines).

in the three-spin system (vide supra). In the case of very strong ν_1^0 and very long τ_{off}, the stepwise features, corresponding to the changes in the regime of state correlation, are very well pronounced, see Figure 4(a). When ν_1^0 is reduced and τ_{off} is taken shorter, the stepwise features broaden and exhibit a more complex shape but the general behavior stays qualitatively the same: Net polarization of spins and polarization transfer to spin 3 are feasible (see Figure 4(b)).

III. EXPERIMENTAL

A. Chemicals

Ethyl phenylpropiolate and styrene were bought from Sigma Aldrich. Catalyst [1,4-bis(diphenylphosphino)butane] (1,5-cyclooctadiene)rhodium(I) tetrafluoroborate was purchased from ABCR GmbH; methanol-d_4 used as a solvent was bought from Deutero GmbH.

B. Hydrogenation

Ethyl phenylpropiolate (20 μl) or phenylacetylene (20 μl) were dissolved in methanol-d_4 (600 μl). The catalyst [Rh(COD)(dppb)]BF_4 (1 mg) was dissolved before adding the substrate. Hydrogenation reactions leading to the formation of PHIP effects are shown in Scheme 1; we used molecules having two or three coupled protons. Hydrogenation was carried out in a 5 mm NMR sample tube directly inside the NMR probehead by purging the hydrogen gas enriched in its para-isomer. Para-hydrogen was prepared by a Bruker parahydrogen generator, the content of para-H_2 was about 92%. A thin plastic capillary was inserted into the NMR tube from top to perform bubbling; the gas pressure for bubbling was about 0.2 bar. The process of bubbling was controlled by a NMR pulse program by means of transistor-transistor logic (TTL)-controlled magnetic valves (GSR Ventiltechnik GmbH).

C. Experimental protocol

PHIP experiments were done using the protocol shown in Figure 1. We used the following typical settings for

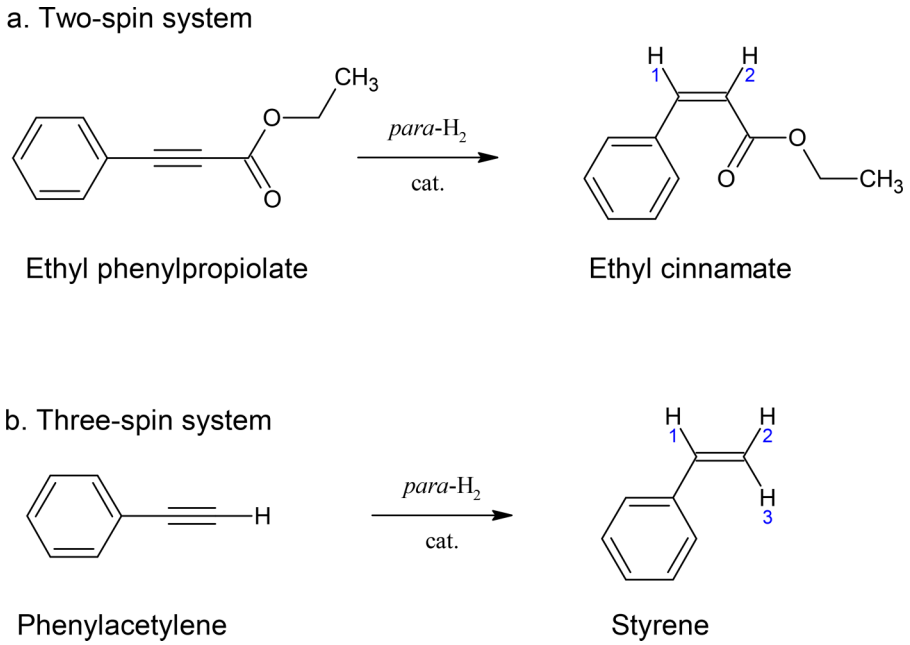

SCHEME 1. Scheme of chemical reactions used to generate PHIP: (a) hydrogenation of ethyl phenylpropiolate leading to the formation of ethyl cinnamate with two polarized protons and (b) hydrogenation of phenylacetylene leading to the formation of styrene with three coupled protons. In both cases, protons 1 and 2 are originating from parahydrogen.

experimental timing. Between subsequent experiments, we introduced a sufficiently long delay to let relax the spins polarized during the previous experiment; typically it was 60 s. The time of bubbling, τ_{bubble}, with parahydrogen was 15 s; the spin-locking RF-field was sustained during $\tau_{SL} = 15$ s and turned off within τ_{off}, which was varied over a wide range. Finally, a RF-pulse was applied to obtain the FID; the NMR spectrum was obtained as the Fourier transform of the FID signal. For detection, we used RF-pulses with $\pi/4$ or $\pi/2$ flip angles. The PHIP spectra were compared with the corresponding PASADENA spectra recorded using $\pi/4$ pulses. We also performed experiments with reduced spectral resolution. This has been done by varying the current in NMR shimming coils. Thus, experiments were done with NMR linewidths from 2 Hz to 130 Hz; the full width at half height of a NMR line was taken as a measure of the linewidth.

IV. RESULTS AND DISCUSSION

A. Conditions for adiabatic variation of the Hamiltonian

First of all, we have run a series of measurements in order to elucidate the experimental parameters compatible with adiabatic variation of the Hamiltonian in the rotating frame. In these measurements, we used different time profiles for $\nu_1(t)$ and varied the RF fading time, τ_{off}. Experiments were performed for polarized ethyl phenylpropiolate, i.e., for a two-spin system. The RF-frequency was chosen such that PHIP was converted to positive net polarization, specifically, we used $\nu_{rf} = 6.4$ ppm. The experimental results were supported by calculations.

The experimental PHIP spectra are shown in Figure 5. One can see that for sufficiently long τ_{off}, the spins indeed become net-polarized (polarization of both spins is the same and positive). At very short RF fading times, net polarization is reduced and spectral lines exhibit unusual behavior: there are dispersive components of the NMR lines. From our previous study, Ref. 33, we know that such components arise from zero-quantum spin coherences (coherence between the $|\alpha\beta\rangle$ and $|\beta\alpha\rangle$ states) generated by non-adiabatic fading of the RF-field. We would like to stress that such unusual signal shape is coming not from improper phasing of the spectra: it is really the spectral pattern characteristic of this particular type of spin coherences. Therefore, the presence of dispersive NMR lines is a clear indication that switching is non-adiabatic. As τ_{off} increases, the dispersive components diminish and spins become net-polarized, see Figure 5.

The dependence of total net polarization of the two protons on τ_{off} is shown in Figure 6 for two $\nu_1(t)$ profiles: $\cos^2$

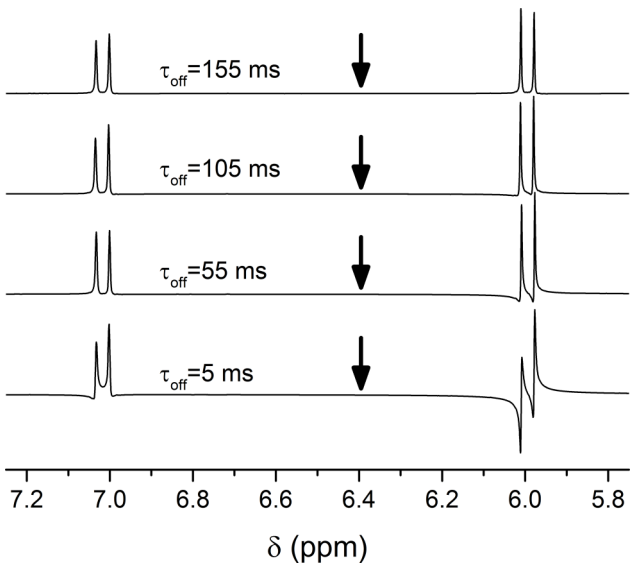

FIG. 5. PHIP spectra of ethyl cinnamate obtained after RF fading with different τ_{off} times (indicated at the spectra). Here, $\nu_1^0 = 3$ kHz, $\nu_{rf} = 6.4$ ppm (indicated by arrows), $\cos^2$-profile was used for RF fading, and NMR flip angle is $\pi/2$. Spectra obtained at short τ_{off} have pronounced dispersive components, in contrast, at long τ_{off} both spins acquire positive net polarization and dispersive components vanish.

and linear profile. In both cases, polarization increases with τ_{off} and saturates at a switching time of about 0.1 s. Experimental results are in good agreement with theoretical simulations. The characteristic time compatible with adiabatic switching is of the order of the inverse J-coupling, $1/J_{12}$; thus, it is relatively short. Although there is no simple expression for the adiabaticity parameters, $\xi_{\mu\nu}$, see Eq. (9), good agreement between the experimental data and simulation encourages us to estimate the degree of adiabaticity from numerical calculations. Since the calculations can be generalized to an arbitrary spin system and arbitrary $\nu_1(t)$ profile, they are capable of evaluating the degree of adiabaticity for a given τ_{off} value.

We also performed experiments for two more profiles of RF-fading, which provide results similar to those shown in Figure 6. These data are presented in the supplementary material.[36]

By analyzing a large array of experimentally measured and calculated spectra for different ν_1^0, τ_{off}, and ν_{rf}, we propose the following procedure for optimizing the performance of the method. First, at other parameters being constant, we obtain a threshold value of ν_1^0, which is sufficient for efficient spin-locking. After that, we start reducing the switching time, τ_{off}. We have found out that for the systems studied here (which are rather typical for PHIP experiments), the threshold ν_1^0 is about 1 kHz: at 0.8 kHz, we obtain 50% of the maximal net polarization and at 2.7 kHz, it is about 90%. Having optimized the ν_1^0 value, we reduced τ_{off} and found out that times of about 60-100 ms are sufficient for good adiabaticity.

B. Two-spin system

The case of two coupled spins was studied in detail in our previous work; different cases corresponding to different ν_{rf} frequencies were discussed and theoretical predictions were compared to experimental data. Here, we demonstrate only one more aspect of PHIP after adiabatic switching of the RF-field. We performed experiments in an inhomogeneous external magnetic field; in this situation, the intensity of lines in the PASADENA spectrum significantly decreases, see Figure 7. This is because the positive and negative NMR lines cancel each other; this effect is most pronounced when the NMR linewidth is above 100 Hz, then the cancellation is almost complete. Line broadening coming from field inhomogeneities can be a problem in many NMR imaging studies, potentially limiting applications of PHIP. As shown below, a remedy is given by manipulating PHIP by adiabatic switching of the RF-field.

Experiments performed for polarized ethyl cinnamate show that, indeed, adiabatic switching of the RF-field enables conversion of the initial singlet spin order into net polarization; in this example, positive net polarization. The conversion works equally well for all the cases shown in Figure 7: PHIP is converted into net polarization, which does not cancel out upon decreasing the spectral resolution. The conversion is efficient even at low spectral resolution; the method thus circumvents the problem of signal cancellation in PHIP. Of course, when line broadening is so strong that the NMR multiplets of protons 1 and 2 overlap, our method does not work. This is because at any setting of the frequency ν_{rf}, we have different regimes of state correlation for different spatial positions in the sample (resulting in different sign of net polarization). However, otherwise the technique solves the problem of signal cancellation coming from overlapping positive and negative lines within the same NMR multiplet.

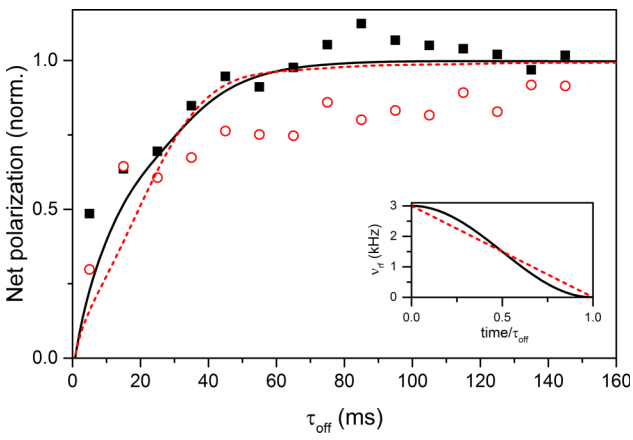

FIG. 6. Net polarization of the two protons of ethyl cinnamate obtained after RF fading with different τ_{off} times. Experimental parameters are $\nu_1^0 = 3$ kHz and $\nu_{rf} = 6.4$ ppm; symbols present experimental results and lines present simulation results. Data are obtained for two different profiles of RF-fading: $\cos^2$-profile (solid black lines and full black squares) and linear profile (dashed red lines and open red circles). Both $\nu_1(t)$ profiles are shown in the inset.

FIG. 7. PHIP spectra of ethyl cinnamate (polarized two-spin system). Here, we show standard PASADENA spectra (obtained without spin-locking, spectra 1, 3, and 5 with anti-phase doublets, shown in black) and spectra obtained after RF fading (spectra 2, 4, and 6 with net polarization of spins, shown in red). Spectra are taken with NMR linewidths of 2 Hz (spectra 1 and 2), 40 Hz (spectra 3 and 4), and 130 Hz (spectra 5 and 6). For detecting spectra 2, 4, and 6, we use the following settings: $\nu_1^0 = 3$ kHz, $\tau_{off} = 1$ s ($\cos^2$-profile was used), and $\nu_{rf} = 6.2$ ppm (indicated by arrows). The NMR flip angle is $\pi/4$ for 1, 3, and 5 and $\pi/2$ for 2, 4, and 6. The signals of residual thermally polarized protons are marked with an asterisk.

C. Three-spin system

To demonstrate that our method is applicable to more general cases, we performed experiments on the three-spin system of the polarized styrene molecule, in which the protons 1 and 2 originating from parahydrogen are coupled to a third proton. In addition, there is weak coupling to the aromatic protons (less than 0.5 Hz); however, in most cases, PHIP transfer to these protons is evanescent.

First of all, we studied the ν_{rf} dependence of the spectral pattern and compared experimental results with calculations. In Figure 8, we show the PHIP spectra obtained for different ν_{rf} frequencies. One can see that it is possible to net-polarize all three spins. For instance, at ν_{rf} = 6.0 ppm, all three signals are absorptive; at ν_{rf} = 6.2 ppm, polarization is predominantly emissive. This behavior is in agreement with the discussion presented in Section II C and in very good agreement with the numerical calculation results. In calculations, no assumptions concerning the speed of RF-field reduction are made: the Liouville-von Neumann equation is solved numerically for the actual $\nu_1(t)$ time profile. In the spectra, we also readily see that polarization is transferred from the primarily polarized spins 1 and 2 to spin 3. This is a consequence of spin mixing under spin-locking conditions where all three spins become strongly coupled so that they can share spin order.

We also ran experiments systematically varying the frequency ν_{rf} and using the WALTZ-16 pulse sequence for spin-locking. In addition, to reveal multiplet polarization of protons, we obtained PHIP spectra using a $\pi/4$ NMR pulse for detection. These data are presented in supplementary material.[36]

Finally, let us demonstrate that by using our method, we gain in the situation where the spectral resolution is low,

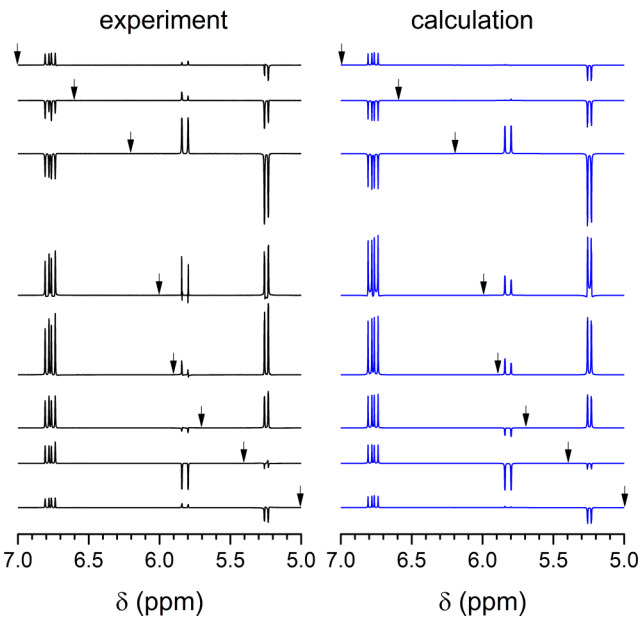

FIG. 8. Experimental (left) and calculated (right) PHIP spectra of styrene. RF-frequency position is shown by arrows and ν_{rf} is (from top to bottom) 7.0, 6.6, 6.2, 6.0, 5.9, 5.7, 5.4, and 5.0 ppm. Spin-locking was done using ν_1^0 = 3 kHz followed by RF fading with τ_{off} = 1 s ($\cos^2$-profile was used). The detection pulse angle is $\pi/2$.

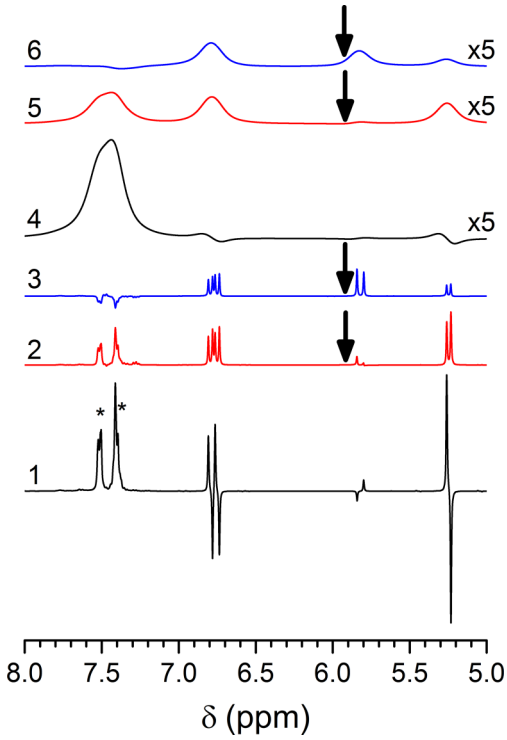

FIG. 9. PHIP spectra of styrene (polarized two-spin system). Here, we show standard PASADENA spectra (obtained without spin-locking, spectra 1 and 4 with anti-phase doublets, shown in black) and spectra obtained after RF fading (spectra 2, 3, 5, and 6 with net polarization of spins). Spectra are taken with NMR linewidths of 2 Hz (spectra 1, 2, and 3) and 70 Hz (spectra 4, 5, and 6). For detecting spectra 2 and 5 (shown in red), we use the following settings: ν_1^0 = 3 kHz, τ_{off} = 1 s ($\cos^2$-profile was used), and ν_{rf} = 5.9 ppm (indicated by arrows); for spectra 3 and 6 (shown in blue), the settings were the same except for spin locking, which has been performed by using the WALTZ16 sequence with the same RF-field strength of 3 kHz. The NMR flip angle is $\pi/4$ for 1, 4 and $\pi/2$ otherwise. The signals of residual thermally polarized protons are marked with an asterisk.

so that in the standard PASADENA experiment positive and negative lines cancel each other. Such results are demonstrated in Figure 9. Whereas in the PASADENA case we obtain the standard spectral pattern (two pairs of anti-phase doublets) by using an adiabatically switched RF-field, it is possible to achieve net polarization of all three protons of styrene; in this example, it is positive net polarization. Reduction of spectral resolution leads to a strong decrease of line intensity in the PASADENA case: the contribution from hyperpolarized spins to the NMR spectrum almost vanishes. In contrast, the method based on adiabatic reduction of the RF-field keeps the same performance: spins remain net polarized and their signals are as strong as in the case of high spectral resolution.

V. CONCLUSIONS

Thus, we have presented a simple method for precise manipulation of spin hyperpolarization, notably, of multiplet polarization. The method is based on preparing polarization in the presence of a spin-locking RF-field, which is subsequently switched off in an adiabatic way; it enables efficient conversion of the singlet spin order into net polarization in a coupled spin

system. Experiments performed for a two-spin system and a three-spin system are in good agreement with the theory outlined in the paper. We systematically studied the conditions required for reaching the desired adiabaticity and proposed a procedure for optimizing the performance of the method. We obtained that for the method, it is appropriate to use RF fading times of about the inverse spin-spin interaction. Furthermore, the method works well even when strong NMR line broadening is present, i.e., the spectral resolution is low. In this situation, the classical PHIP technique suffers from mutual cancellation of positive and negative lines; our method gets around this problem by converting the singlet spin order into positive or negative net polarization of spins.

Although all examples presented here deal with the standard PHIP case, we anticipate that the method is applicable to SABRE, for instance, for converting the spin order of H_2 in the SABRE complex from singlet to triplet (which gives observable NMR signals) and for polarizing nuclei in SABRE substrates. Up to now, it has been demonstrated that high-field SABRE is feasible when the polarized spin system is excited by RF-fields;[8] this idea, in combination with an adiabatic passage through a level crossing in the rotating frame, can be exploited to polarize spin-1/2 heteronuclei by SABRE.[26] We expect that adiabatic correlation in the rotating frame can be used to polarize SABRE substrates. This possibility can open new avenues in SABRE and broaden the range of applications of this technique.

In general, we anticipate that methods using adiabatically switched RF-fields can be very useful for manipulating non-thermal spin order, in particular, multiplet spin order. Such methods can be applied also to multi-spin systems for precise control and conversion of non-thermal spin order. Furthermore, by using two switched RF-fields, it becomes possible to transfer PHIP to hetero-nuclei.[26] Another possible application is dealing with so-called Long-Lived States (LLSs),[39,40] which exploit the symmetry of intramolecular dipolar couplings and persist for time periods much longer than the T_1-relaxation time. Typically, LLSs are the singlet states in pairs of spins; they can be used for storing spin hyperpolarization[41–44] and studying slow dynamic processes.[45–49] Since our method enables efficient conversion between the singlet spin order and longitudinal spin magnetization, we expect that it is highly potent for creating and investigating LLSs.

ACKNOWLEDGMENTS

This work was partially supported by the Russian Foundation for Basic Research (Grant Nos. 14-03-00380 and 15-33-20716); all experimental studies have been done in the framework of Grant No. 15-13-20035 from the Russian Science Foundation.

[1]J. Natterer and J. Bargon, Prog. Nucl. Magn. Reson. Spectrosc. **31**, 293 (1997).
[2]S. B. Duckett and R. E. Mewis, Acc. Chem. Res. **45**, 1247 (2012).
[3]R. A. Green, R. W. Adams, S. B. Duckett, R. E. Mewis, D. C. Williamson, and G. G. R. Green, Prog. Nucl. Magn. Reson. Spectrosc. **67**, 1 (2012).
[4]C. R. Bowers and D. P. Weitekamp, J. Am. Chem. Soc. **109**, 5541 (1987).
[5]M. G. Pravica and D. P. Weitekamp, Chem. Phys. Lett. **145**, 255 (1988).
[6]R. W. Adams, J. A. Aguilar, K. D. Atkinson, M. J. Cowley, P. I. P. Elliott, S. B. Duckett, G. G. R. Green, I. G. Khazal, J. López-Serrano, and D. C. Williamson, Science **323**, 1708 (2009).
[7]A. N. Pravdivtsev, A. V. Yurkovskaya, H.-M. Vieth, K. L. Ivanov, and R. Kaptein, ChemPhysChem **14**, 3327 (2013).
[8]A. N. Pravdivtsev, A. V. Yurkovskaya, H.-M. Vieth, and K. L. Ivanov, Phys. Chem. Chem. Phys. **16**, 24672 (2014).
[9]T. Theis, M. Truong, A. M. Coffey, E. Y. Chekmenev, and W. S. Warren, J. Magn. Reson. **248**, 23 (2014).
[10]F. Reineri, S. Bouguet-Bonnet, and D. Canet, J. Magn. Reson. **201**, 107 (2011).
[11]K. L. Ivanov, M. V. Petrova, N. N. Lukzen, and R. Z. Sagdeev, Dokl. Phys. Chem. **427**, 121 (2009).
[12]J. F. Dechent, L. Buljubasich, L. M. Schreiber, H. W. Spiess, and K. Münnemann, Phys. Chem. Chem. Phys. **14**, 2346 (2012).
[13]L. Buljubasich, I. Prina, M. B. Franzoni, K. Münnemann, H. W. Spiess, and R. H. Acosta, J. Magn. Reson. **230**, 155 (2013).
[14]L. Buljubasich, I. Prina, and R. H. Acosta, J. Phys. Chem. Lett. **4**, 3924 (2013).
[15]A. N. Pravdivtsev, K. L. Ivanov, A. V. Yurkovskaya, H.-M. Vieth, and R. Z. Sagdeev, Dokl. Phys. Chem. **465**, 267 (2015).
[16]A. S. Kiryutin, K. L. Ivanov, A. V. Yurkovskaya, H.-M. Vieth, and N. N. Lukzen, Phys. Chem. Chem. Phys. **15**, 14248 (2013).
[17]G. C. Chingas, A. N. Garroway, W. B. Moniz, and R. D. Bertrand, J. Am. Chem. Soc. **102**, 2526 (1980).
[18]S. Hediger, B. H. Meier, N. D. Kurur, G. Bodenhausen, and R. R. Ernst, Chem. Phys. Lett. **223**, 283 (1994).
[19]P. Pelupessy and E. Chiarparin, Concepts Magn. Reson. **12**, 103 (2000).
[20]P. Hodgkinson and A. Pines, J. Chem. Phys. **107**, 8742 (1997).
[21]M. H. Levitt, J. Chem. Phys. **94**, 30 (1991).
[22]P. Hodgkinson, C. Auger, and L. Emsley, J. Chem. Phys. **109**, 1873 (1998).
[23]T. R. Eykyn, F. Ferrage, E. Winterfors, and G. Bodenhausen, ChemPhysChem **1**, 217 (2000).
[24]N. D. Kurur and G. Bodenhausen, J. Magn. Reson., Ser. A **114**, 163 (1995).
[25]G. Zandomeneghi and B. H. Meier, J. Biomol. NMR **30**, 303 (2004).
[26]A. N. Pravdivtsev, A. V. Yurkovskaya, N. N. Lukzen, K. L. Ivanov, and H.-M. Vieth, J. Phys. Chem. Lett. **5**, 3421 (2014).
[27]A. N. Pravdivtsev, A. V. Yurkovskaya, N. N. Lukzen, H.-M. Vieth, and K. L. Ivanov, Phys. Chem. Chem. Phys. **16**, 18707 (2014).
[28]A. J. Shaka, J. Keeler, T. Frenkiel, and R. Freeman, J. Magn. Reson. (1969-1992) **52**, 335 (1983).
[29]A. J. Shaka, J. Keeler, and R. Freeman, J. Magn. Reson. (1969-1992) **53**, 313 (1983).
[30]S. E. Korchak, K. L. Ivanov, A. V. Yurkovskaya, and H.-M. Vieth, Phys. Chem. Chem. Phys. **11**, 11146 (2009).
[31]E. Vinogradov and A. K. Grant, J. Magn. Reson. **194**, 46 (2008).
[32]A. Messiah, *Quantum Mechanics* (North-Holland Publishing Company, Amsterdam, 1965).
[33]E. A. Nasibulov, A. N. Pravdivtsev, A. V. Yurkovskaya, N. N. Lukzen, H.-M. Vieth, and K. L. Ivanov, Z. Phys. Chem. **227**, 929 (2013).
[34]S. Schäublin, A. Hoehener, and R. R. Ernst, J. Magn. Reson. (1969-1992) **13**, 196 (1974).
[35]R. R. Ernst, G. Bodenhausen, and A. Wokaun, *Principles of Nuclear Magnetic Resonances in One and Two Dimensions* (Clarendon Press, Oxford, 1978).
[36]See supplementary material at http://dx.doi.org/10.1063/1.4937392 for theoretical analysis of a two-spin system and additional figures.
[37]H. Jóhannesson, O. Axelsson, and M. Karlsson, C. R. Phys. **5**, 315 (2004).
[38]K. L. Ivanov, A. V. Yurkovskaya, and H.-M. Vieth, Z. Phys. Chem. **226**, 1315 (2012).
[39]G. Pileio, Prog. Nucl. Magn. Reson. Spectrosc. **56**, 217 (2010).
[40]M. H. Levitt, Annu. Rev. Phys. Chem. **63**, 89 (2012).
[41]P. Ahuja, R. Sarkar, S. Jannin, P. R. Vasos, and G. Bodenhausen, Chem. Commun. **46**, 8192 (2010).
[42]M. B. Franzoni, L. Buljubasich, H. W. Spiess, and K. Münnemann, J. Am. Chem. Soc. **134**, 10393 (2012).
[43]G. Pileio, S. Bowen, C. Laustsen, M. C. D. Tayler, J. T. Hill-Cousins, L. J. Brown, R. C. D. Brown, J. H. Ardenkjaer-Larsen, and M. H. Levitt, J. Am. Chem. Soc. **135**, 5084 (2013).
[44]P. R. Vasos, A. Comment, R. Sarkar, P. Ahuja, S. Jannin, J.-P. Ansermet, J. A. Konter, P. Hautle, B. van den Brandt, and G. Bodenhausen, Proc. Natl. Acad. Sci. U. S. A. **106**, 18469 (2009).

[45]A. Bornet, P. Ahuja, R. Sarkar, L. Fernandes, S. Hadji, S. Y. Lee, A. Haririnia, D. Fushman, G. Bodenhausen, and P. R. Vasos, ChemPhysChem **12**, 2729 (2011).
[46]R. Buratto, D. Mammoli, E. Chiarparin, G. Williams, and G. Bodenhausen, Angew. Chem., Int. Ed. **53**, 11376 (2014).
[47]S. Cavaldini and P. R. Vasos, Concepts Magn. Reson., Part A **32A**, 68 (2008).
[48]G. Pileio, J.-N. Dumez, I.-A. Pop, J. T. Hill-Cousins, and R. C. D. Brown, J. Magn. Reson. **252**, 130 (2015).
[49]R. Sarkar, P. R. Vasos, and G. Bodenhausen, J. Am. Chem. Soc. **129**, 328 (2007).